Supplementary information

A Zwitterionic-Enabled One-Pot Electrochemical Strategy for Stable End-Point Detection of Isothermal Nucleic Acid Amplification

Yijie Wang[a, 1], Yang Li[a, 1], Jiufa Zhang[a], Mingjun Cai[a], Qi Fu[a], Xiaohan Lin[a], Cuiping Ma[b], Chao Shi[a, c *]

[a] *Qingdao Nucleic Acid Rapid Testing International Science and Technology Cooperation Base, College of Life Sciences, Qingdao University, Qingdao, 266071, P. R. China.*

[b] *Sino-UAE International Cooperative Joint Laboratory of Pathogenic Microorganism Rapid Detection, Qingdao Nucleic Acid Rapid Detection Engineering Research Center, Qingdao Key Laboratory of Nucleic Acid Rapid Detection, College of Biological Engineering, Qingdao University of Science and Technology, Qingdao, 266042, P. R. China.*

[c] *Qingdao Navid Biotechnology Co., Ltd, Qingdao, 266114, P. R. China*

[*] To whom correspondence should be addressed.

[1] These two authors contributed equally to this work

Tel (Fax): +86-532-85955399

E-mail: sc169@163.com

Table·S1. Sequences of nucleic acids used in this work

Name		Sequence (5'-3')
LAMP	F3	ATGCAAAGAAAATTGAAGTCGA
	B3	GCGTTGTCTTCGCTCCAAAT
	FIP	CGTTTACCATTTTTCCATCAGCATAGTTTGACAAAGGTCAAAGAACT
	BIP	TCAAGGCTTGGCTAAAGTTGCTTATTTTCGCTTGTGCTTCACTT
	LF	TACGCTAAGCCACGTCCATA
	LB	CCTAACAATACACATGAACAAC
PCR	F	AGCGATTGATGGTGATACGGT
	R	AGGATGCTTTGTTTCAGGTGT

Notes: LAMP primer sequences were adopted from previously published studies[1]. PCR primers were designed and optimized using NUPACK software (http://www.nupack.org/) and NCBI Primer-BLAST (https://www.ncbi.nlm.nih.gov/tools/primer-blast).

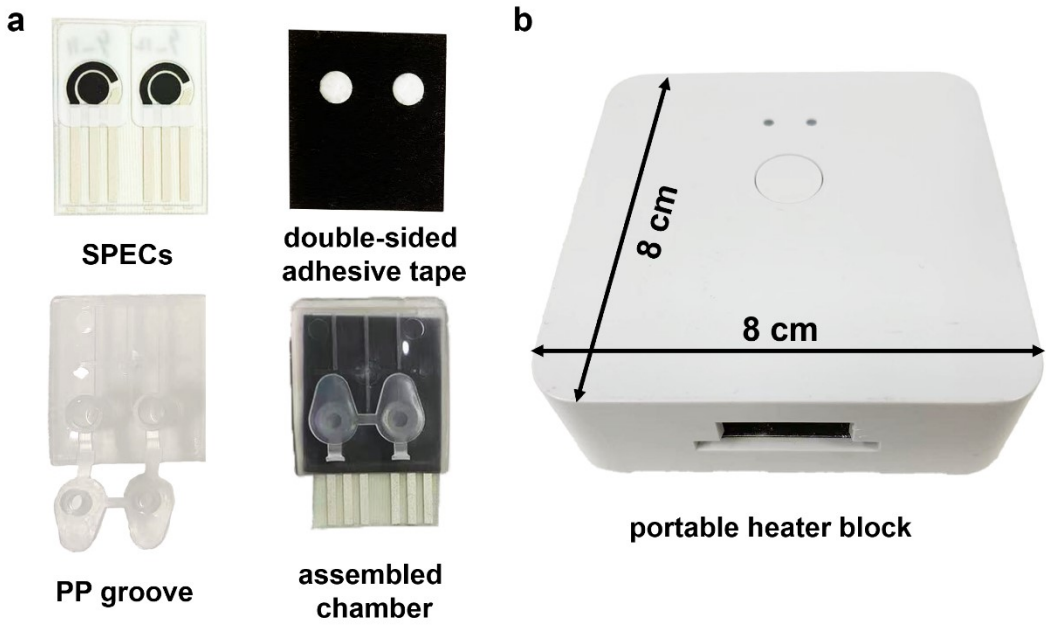

Figure S1. Assembly and configuration of the portable EC-LAMP system. (a) Fabrication of the reaction chamber by integrating SPCEs, a PP groove, and double-sided adhesive tape. (b) Portable heater block employed for isothermal incubation during in situ EC-LAMP.

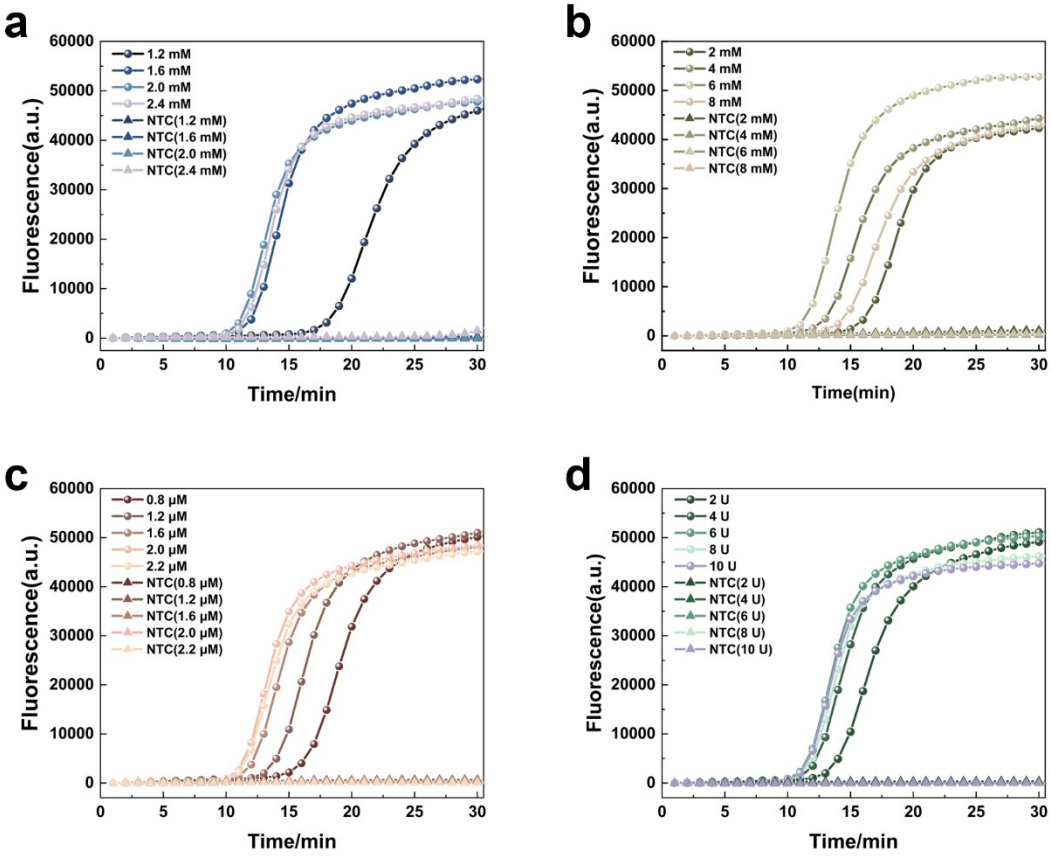

Figure S2. Optimization of the reaction conditions for LAMP. (a) different amounts of dNTPs. (b) different amounts of $MgSO_4$. (c) different amounts of inner primers (FIP/BIP). (d) different amounts of Bst DNA polymerase.

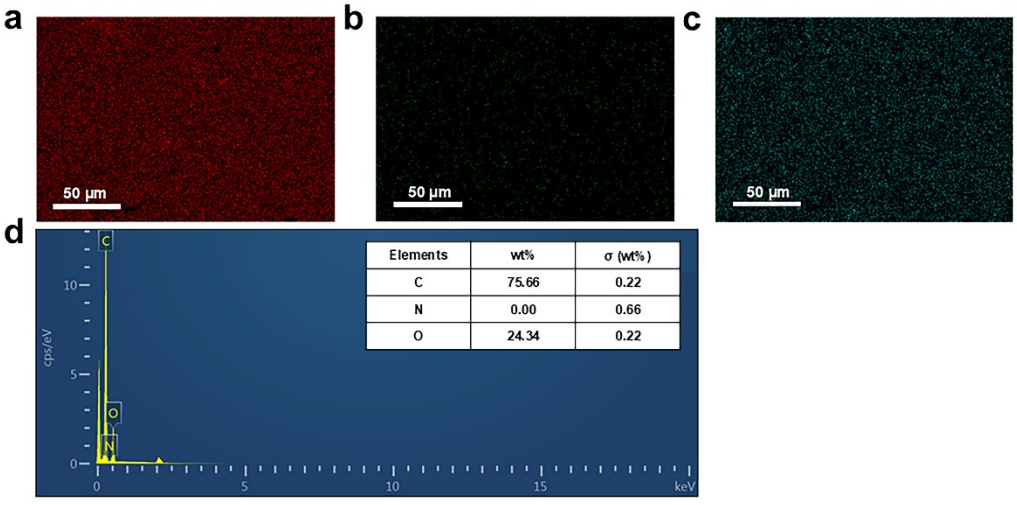

Figure S3. (a–c) EDS elemental mapping images of C, N, and O, respectively, of the bare electrode. (d) EDS spectrum of the selected area, showing the characteristic peaks of C, N, and O. The inset table lists the corresponding elemental weight percentages (wt%) with standard deviations (σ).

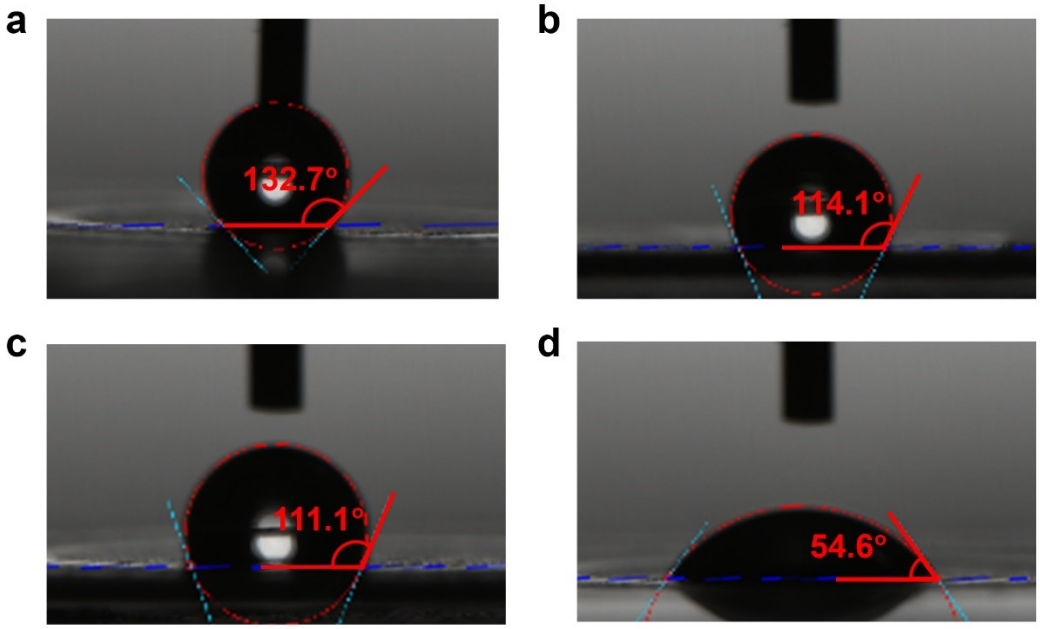

Figure S4. Water contact angle images of the electrode surfaces: (a) bare SPCE, (b) H_2SO_4-treated SPCE, (c) EDC/NHS-treated SPCE, and (d) PCBMA- SPCE.

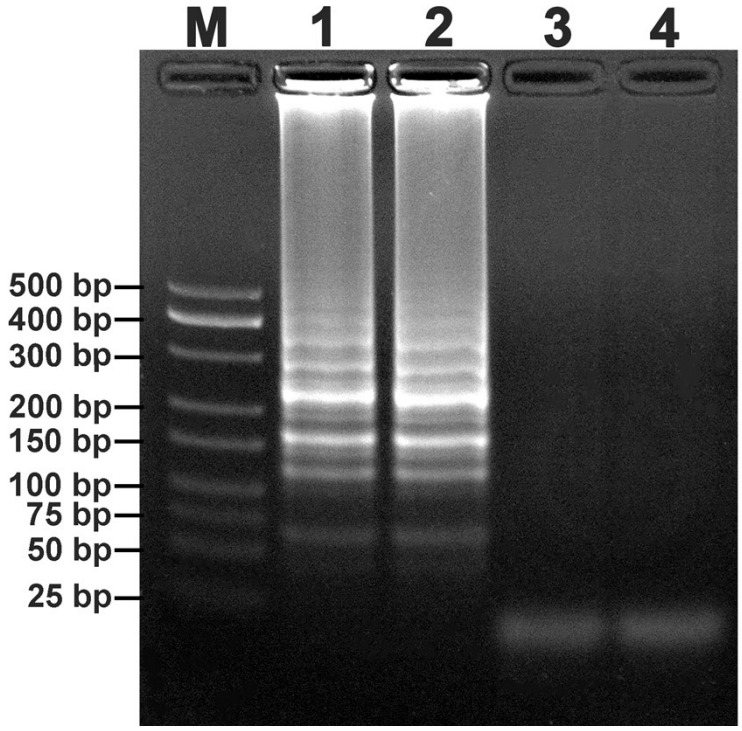

Figure S5. Agarose gel electrophoresis image of the LAMP products. Lane 1, Real-time fluorescence LAMP positive; Lane 2, In situ electrochemical LAMP positive; Lane 3, Real-time fluorescence LAMP NTC; Lane 4, In situ electrochemical LAMP NTC. M represents the DNA Marker (25–500 bp). The target concentration was 10^6 CFU/mL. NTC stands for no target control.

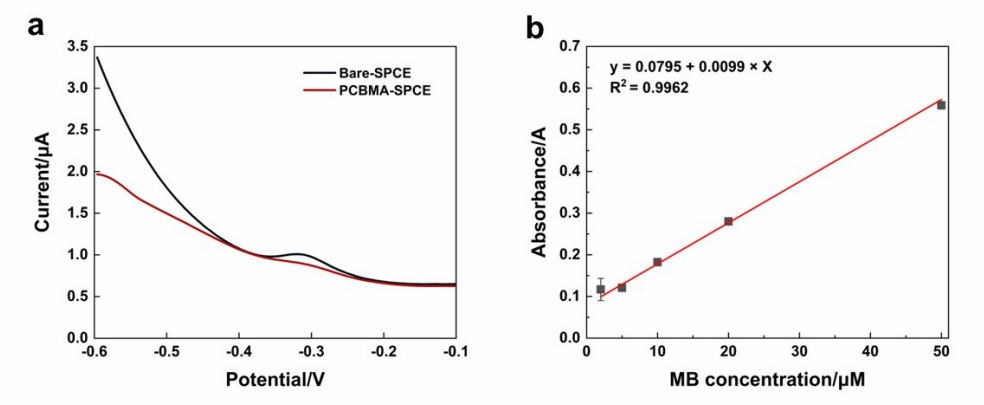

Figure S6. Quantitative evaluation of MB adsorption. (a) Electrochemical signals of residual MB on bare and PCBMA-modified electrodes measured in PBS after removal of MB solution and triple rinsing. (b) Calibration curve of MB absorbance versus concentration used for quantification. Error bars represent standard deviations from three independent measurements.

To quantitatively evaluate the nonspecific adsorption of methylene blue (MB), the residual MB concentration in the supernatant after incubation with the electrodes was determined using a calibration curve (Figure S6b). Based on the Beer–Lambert law, the absorbance values were converted to concentration using the linear relationship A = 0.0795 + 0.0099C. After 30 min incubation with an initial MB concentration of 20 μM, the remaining concentration (C_e) was calculated to be 19.90 μM for the PCBMA-modified electrode and 19.46 μM for the bare electrode. Accordingly, the adsorption amount ($q = C_0 - C_e$) was estimated to be 0.10 μM and 0.54 μM for PCBMA and bare electrodes, respectively. These results indicate that the PCBMA-modified surface significantly suppresses MB adsorption. The adsorption mitigation efficiency was calculated to be approximately 81.5%, demonstrating the effective antifouling property of the zwitterionic PCBMA coating. Although the concentration difference is relatively small, the trend is consistent with electrochemical measurements.

Table S2. Comparison of representative electrochemical LAMP (EC-LAMP) systems reported for nucleic acid detection.

Signal rationale	Electrode / Interface	Antifouling strategy	Time	Sensitivity	Target	References
Potentiometric pH change	Hydrated iridium oxyhydroxide-modified SPCEs	Not found	30 min	~1.0 × 10^3 CFU/mL	*Vibrio parahaemolyticus*	2
Oxidation of phenol red (pH-dependent)	thick-film carbon electrodes	Not found	122 min	~2×10^5 copies/μL	*Streptococcus pneumoniae*	3
pH change via cresol red	3D-printed electrode with pH-responsive readout	UV-laser surface treatment	31 min	~11 copies/μL	Methicillin-resistant *S. aureus*	4
Phenol red	SPE	Not found	30 min	20 copies /μL	*SARS-CoV-2*	5
pH change	graphene–gold–polyaniline (Gr/Au/PANI) electrode	Not found	>30 min	1 copy/μL	*Helicobacter pylori*	6
pH change	polyaniline	Not found	30 min	1 copy/ reaction	*Mycoplasma pneumoniae*	7
Potentiometric pH change	3D printed electrode - modified iridium oxide layer	Not found	>60 min	100 copies/mL	lambda DNA	8
Mediator-	Carbon	Covalent	30 min	~1×10^3/4×10^2	*Staphylococc*	9

displacement MB labeled mediator	electrode + solid-phase universal probe	probe attachment reduces nonspecific		copies/reaction	*us aureus*/ *Treponema pallidum*	
Molybdophosphate precipitate	Multiwalled carbon nanotubes - modified GCE	Not found	70 min	~17 fg/μL	*Nosema bombycis*	10
molybdophosphate precipitate	SPCEs	Not found	45 min	~1.0×10^3 CFU/mL 5.29 copies/μL	SARS-CoV-2	11
Digoxigenin-dUTP	Carbon electrode chips	Not found	110 min	Not found	PCA3 lncRNA	12
Hoechst 33258	a disposable electrochemical printed (DEP) chip	Not found	60 min	3×10^2 copies/reaction	GMO	13
RuHex	gold electrode	Not found	60 min	10^1 copies	plasmid DNA (parvovirus VP2 gene)	14
Malachite green	Thick-film screen printed electrodes	Not found	30 min	~22 copies/μL	SARS-CoV-2	15
Methylene blue	AuNPs/SH-DNA probe/	Pyrene	40 min	~17.7 CFU/mL	*Salmonella enteritidis*	16
Methylene blue	SPCEs	Not found	30 min	~2.5×10^{-6} ng/μL	SARS-CoV-2	17
Methylene blue	PCBMA-modified SPCEs	PCBMA	30 min	12 CFU/mL	*Staphylococcus aureus*	This work

71
72

Table S3. Determination of *S. aureus* in milk samples with the proposed biosensor.

Spiked concentration (CFU mL^{-1})	Found concentration (CFU mL^{-1}) [#]	Recovery (%)	RSD (%)
1.0×10^2	9.04×10^1	90.4	0.66
1.0×10^4	9.18×10^3	91.8	1.44
1.0×10^6	9.69×10^5	96.9	2.13

[#]Average of three measurements

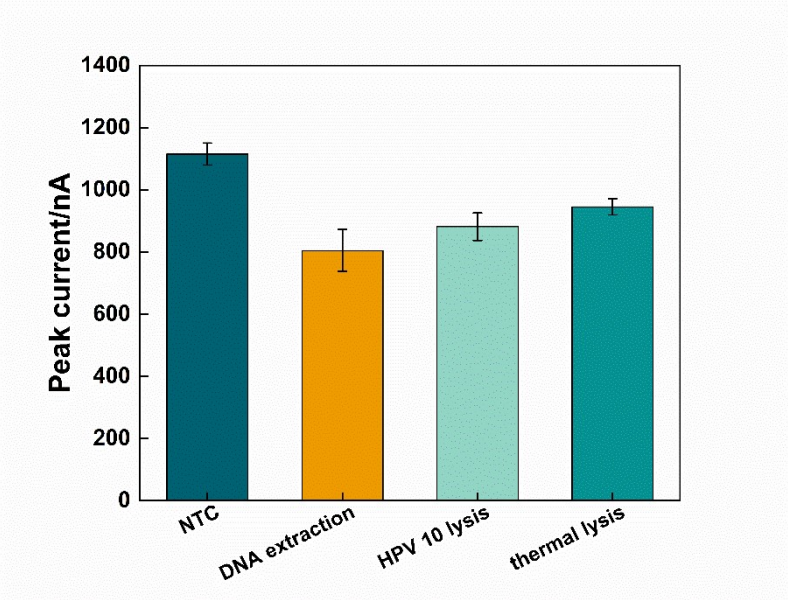

Figure S7. Electrochemical responses obtained from spiked milk samples (10^3 CFU mL^{-1}) subjected to different pretreatment methods. NTC: no-template control; DNA extraction: commercial kit-based purification; nucleic acid releaser (95°C, 5 min); thermal lysis: direct heating (95°C, 5 min).

References

1 Y. Wang, H. Li, Y. Wang, L. Zhang, J. Xu and C. Ye, *Front. Microbiol.*, 2017, **8**, 192.

2 L. Tian, Y. Li, H. Wang, X. Li, Q. Gao, Y. Liu, Y. Liu, Q. Wang, C. Ma and C. Shi, *Anal. Biochem.*, 2024, **693**, 8.

3 A. Gonzalez-Lopez, M.D. Cima-Cabal, P. Rioboo-Legaspi, E. Costa-Rama, M.D.M. Garcia-Suarez and M.T. Fernandez-Abedul, *Anal. Chem.*, 2022, **94**, 13061-13067.

4 L.F. de Lima, P.F.N. Estrela, L.C. Faustino, J. Souza, E.T.S. Geroncio, L.F. de Lima, E.F.L.C. Bailao, W.R. de Araujo, T.R.L.C. Paixao and G.R.M. Duarte, *Anal. Chim. Acta*, 2025, **1372**, 9.

5 P. Rioboó-Legaspi, E. Costa-Rama and M.T. Fernández-Abedul, *Lab Chip*, 2024, **24**, 4085-4095.

6 R.R. Kumar, C.Y. Wang, A.M. Bharti, W.C. Hu, Y.C. Zhang, L.S. Yu, P. Tungtrakarnkul, K.C.W. Wu and C.H. Chuang, *Anal. Chem.*, 2025.

7 H. Wang, Y. Li, L. Tian, X. Li, Q. Gao, Y. Liu, C. Ma, Q. Wang and C. Shi, *Analytical Methods : Advancing Methods and Applications*, 2024, **16**, 3020-3029.

8 Z. Xu, K. Yin, X. Ding, Z. Li, X. Sun, B. Li, R.V. Lalla, R. Gross and C. Liu, *Biosens. Bioelectron.*, 2021, **186**, 113306.

9 M. Trotter, A. Schreiber, D. Kleinknecht, Z. Bagherian, F. von Stetten and N. Borst, *ACS Sens.*, 2024, **10**, 1788-1796.

10 S. Xie, Y. Yuan, Y. Chai and R. Yuan, *Anal. Chem.*, 2015, **87**, 10268-10274.

11 K. Borah Slater, M. Ahmad, A. Poirier, A. Stott, B.S. Siedler, M. Brownsword, J. Mehat, J. Urbaniec, N. Locker, Y. Zhao, R. La Ragione, S.R.P. Silva and J. McFadden, *Iscience*, 2023, **26**, 107570.

12 L. Moranova, M. Stanik, R. Hrstka, S. Campuzano and M. Bartosik, *Talanta*, 2022, **238**, 123064.

13 M.U. Ahmed, M. Saito, M.M. Hossain, S.R. Rao, S. Furui, A. Hino, Y. Takamura, M. Takagi and E. Tamiya, *The Analyst*, 2009, **134**, 966-972.

14 K. Hashimoto, M. Inada and K. Ito, *Anal. Biochem.*, 2017, **539**, 113-117.

15 P. Rioboó-Legaspi, N. Rabanal-Rubio, E. Costa-Rama, M.D. Cima-Cabal, M.D.M. García-Suárez and M.T. Fernández-Abedul, *Microchem J.*, 2024, **198**, 110172.

16 X. Li, Y. Fan, H. Gong, H. Wang, Y. Ji, L. Xu, C. Ma and C. Shi, *Mikrochim. Acta*, 2024, **191**, 11.

17 R.G. Ramírez-Chavarría, E. Castillo-Villanueva, B.E. Alvarez-Serna, J. Carrillo-Reyes, R.M. Ramírez-Zamora, G. Buitrón and L. Alvarez-Icaza, *J. Environ. Chem. Eng.*, 2022, **10**, 107488.